Dynamics of air–sea carbon dioxide fluxes and their trends in the global context

K. Lekshmi, Rishikesh Bharti* and Chandan Mahanta

Department of Civil Engineering, Indian Institute of Technology Guwahati, Guwahati 781 039, India

This article reviews the dynamics of CO_2 fluxes in the global scenario. Most of the available techniques for sea-surface CO_2 partial-pressure estimation are regional models that depend on the key regulating parameters of partial pressures. Global-scenario of fluxes reveals a contrasting trend, indicating subpolar- and polar-waters dominated by physical forcings in winter, releasing CO_2 whereas a biological drawdown of atmospheric CO_2 in summer. In the tropical oceans, thermal-regulation weakens biological forcing leading to influx in winter and outflux in summer. The Atlantic Ocean acts as an intense sink (–815 to –1295 mmol C m^{-2} yr^{-1}); the strong source in the Pacific-equatorial belt is balanced by temperate sinks. The Indian Ocean as a whole acts as a sink (-8.41×10^{15} mmol C yr^{-1}) whereas the northwestern sub-basin acts as a source (2.04×10^{15} mmol C yr^{-1}). The net global ocean uptake is 50×10^{15} mmol C yr^{-1} where the physical- and biological-forcings along with seasonality play crucial roles in the flux direction.

Keywords: Carbon dioxide fluxes, earth system, global scenario, ocean–atmosphere interface, seasonal variability.

CARBON dioxide (CO_2) though constitutes only a minor fraction (0.04%) of the volume of air, is the highest contributing greenhouse gas (GHG) to global warming, thus acting as one of the major factors in the radiative climate forcing[1]. CO_2 gas emissions contribute about 77% of the anthropogenic GHG emissions and 63% of the direct radiative forcing[2]. About 50% of this added CO_2 concentration in the atmosphere is being absorbed by the oceans, serving as the global CO_2 storage. The role of oceans in regulating the global climate is significantly affected by the spatial and seasonal variations in the CO_2 gas exchange process at the marine–atmosphere interface (Figure 1). Analysis of the regional controls on the direction of these fluxes is important in understanding the capacity of various oceanic regions in balancing the global CO_2 concentrations[3,4]. CO_2 flux can be divided into two constituents; the exchange of natural CO_2 and the uptake of anthropogenic CO_2 emissions. CO_2 is released to the atmosphere from natural sources like biological respiration, organic decomposition, volcanic activities and chemical weathering as well as man-made sources like land-use change, cement production and fossil-fuel burning associated with manufacturing and industry, households and public buildings, and transport[2,5].

The CO_2 dissolved in the ocean occurs mainly in three inorganic forms, namely free aqueous carbon dioxide (CO_{2aq}), bicarbonate ion (HCO_3^-) and carbonate ion (CO_3^{2-}), where HCO_3^- represents majority of the ocean inorganic carbon. The chemistry of this process as given in the literature[4,6] is shown in eqs (1)–(4). A minor percentage of the diffused CO_2 exists as carbonic acid which is about 0.3% of the aqueous CO_2

$$CO_2(g) \rightarrow CO_2(aq), \quad (1)$$

$$CO_2(aq) + H_2O(l) \leftrightarrow H_2CO_3(aq), \quad (2)$$

$$H_2CO_3 \leftrightarrow H^+ + HCO_3^-, \quad (3)$$

$$HCO_3^- \leftrightarrow H^+ + CO_3^{2-}. \quad (4)$$

These interspecies transitions occur in favour of maintaining a constant oceanic pH, thereby acting as a buffer system. Such dissolved CO_2 in the surface ocean layer is transported into deeper layers through physical and biological carbon pumps, which reduces the surface water carbon dioxide partial pressures (pCO_2) so as to enhance further uptake of atmospheric CO_2 (Figure 2). The physical pump functions through downward mixing and downwelling processes and the biological pump involves gravitational settling of the fixed surface water carbon in biogenic debris. The physical pump also helps in maintaining the surface water pCO_2 balance through upwelling of CO_2-rich deep waters[1].

Importance of the ocean–atmospheric CO_2 fluxes

Studies have been carried out globally to understand the factors and mechanisms that govern the air–sea exchange of CO_2. The concentration of CO_2 gas in the atmosphere and ocean surface is the chief factor governing the flux direction[3,4]. This concentration is regulated by the physical, chemical and biological processes in the marine environment. These processes and their impacts vary regionally and seasonally, thereby impacting the spatial and seasonal trends in the CO_2 fluxes. Even though the global ocean acts as a net CO_2 sink, the regional fluctuations in the

*For correspondence. (e-mail: rbharti@iitg.ac.in)

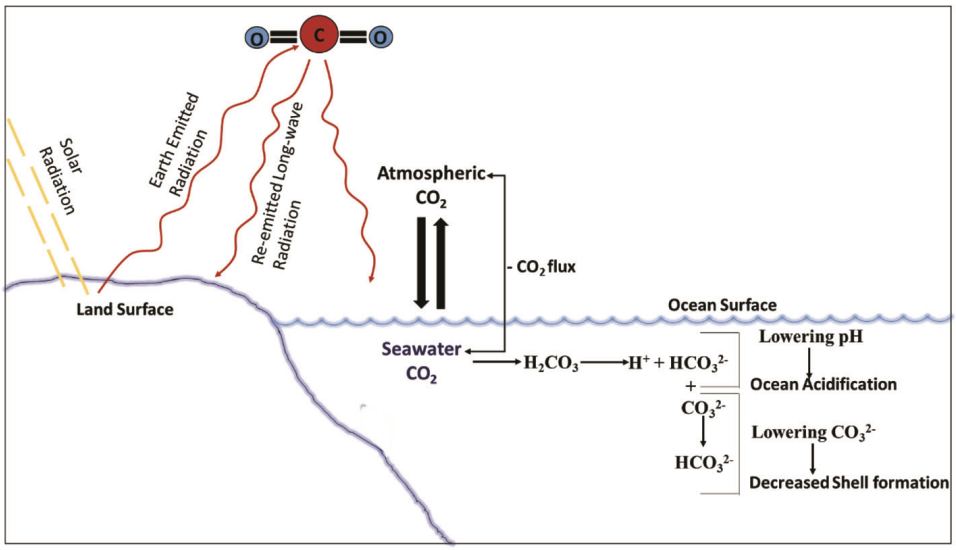

Figure 1. Carbon dioxide (CO_2) gas exchange process within the earth systems.

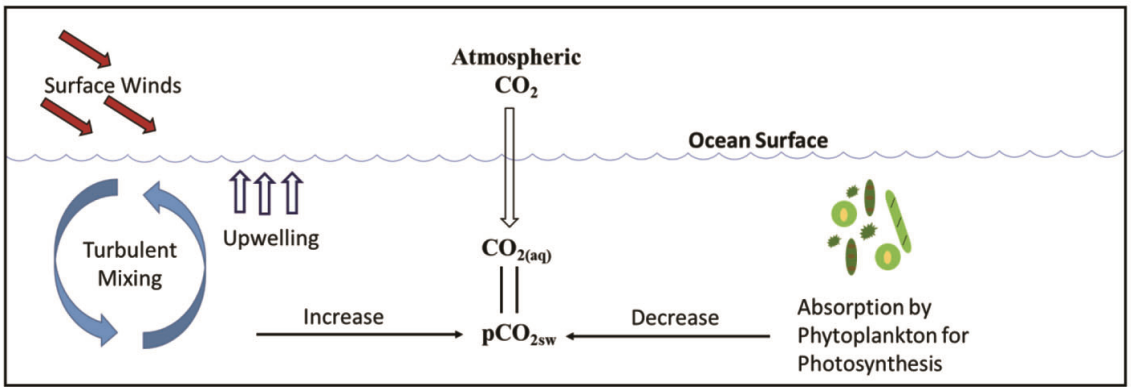

Figure 2. Physical and biological CO_2 pump regulating pCO_2 at the marine–atmosphere interface.

CO_2 exchange have potential repercussions on the global trends of CO_2 fluxes[3]. The ocean–atmosphere interactions and their vital role in the regulation of global biogeochemical cycles significantly contribute to the global climate system. Such natural cycles are continuously being interrupted by anthropogenic activities such as emission of GHGs like CO_2 and other lethal trace gases. Analysis of the transport, transformation and recycling of stored carbon in the ocean is essential in understanding carbon cycling in the marine–atmospheric system and thereby its significance in the global climate[7].

The ongoing reduction of ocean pH following the uptake of atmospheric CO_2 is referred to as ocean acidification, where the increase in the oceanic CO_2 leads to a decrease in the carbonate ion and increase in bicarbonate ion concentration. Such reduction in the carbonate concentration results in the reduction of $CaCO_3$ stability, leading to the deficiency of $CaCO_3$ for the marine calcifying organisms[4,8]. The ocean serves as the major reservoir of anthropogenic CO_2 as it holds about 93% of the carbon compared to the other reservoirs. Effective regulations for GHG emissions require accurate modelling of the global carbon cycle to understand the role of the ocean as the global CO_2 sink[4].

Carbon dioxide partial pressures as indicators of CO_2 fluxes

The CO_2 flux is primarily defined by the CO_2 gas transfer velocity, seawater solubility of CO_2 and the difference in the CO_2 partial pressures at the sea surface and the air above, represented as δpCO_2. Among these, pCO_2 is the thermochemical steering factor for the net air–sea CO_2 flux, determining the flux direction at the ocean–atmospheric interface. Compared to atmospheric pCO_2, spatial and seasonal fluctuations are more prominent in the seawater pCO_2, making it the principal factor in flux determination[1,9].

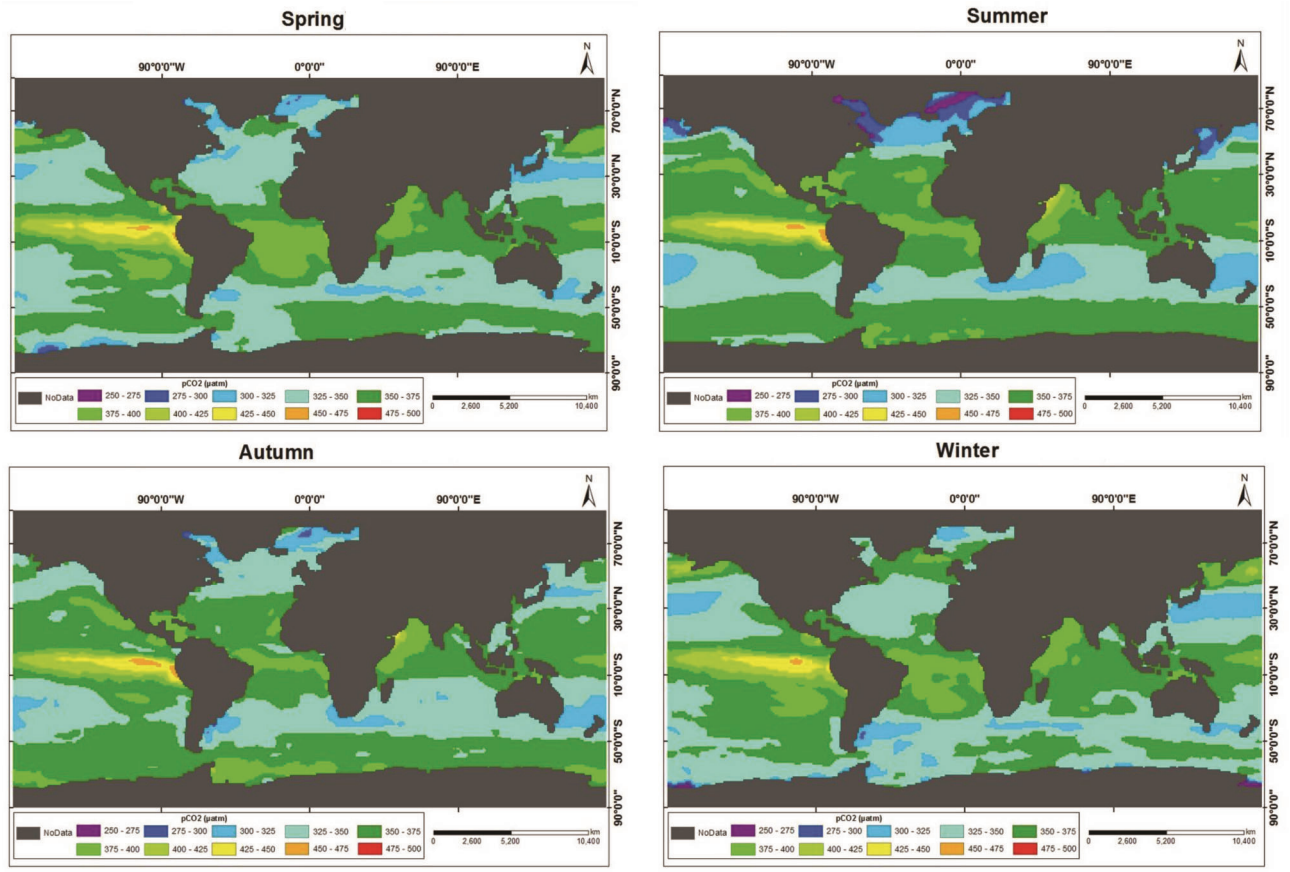

Figure 3. Seasonal variability of global pCO_2.

Accuracy of the CO_2 flux estimation thus depends on the spatio-temporal resolution of the measured pCO_2. Efforts have been made worldwide to obtain pCO_2 with better resolution using buoys and ship-board measurements. However, the spatial resolution of the present measurement network is far coarser (<250 km grid), which emphasizes the need for improved extrapolation techniques[10]. Subsequently Landschutzer *et al.*[11] have generated observational-based global monthly gridded sea-surface pCO_2 from 1982 to 2015. Figure 3 represents the seasonal pCO_2 map in the global context[11]. The maximum value observed in the equatorial Pacific Ocean in all the seasons ranges between 450 and 475 µatm, whereas the Arctic Ocean exhibits minimum values ranging from 250 to 275 µatm in summer. In addition, low pCO_2 values (275–300 µatm) were observed in the Southern Ocean in the spring and winter seasons.

Estimation of carbon dioxide partial pressures of seawater

The seawater partial pressures are primarily regulated by thermal variations and biologically induced CO_2 concentration changes in the water, while other important factors acting in combination with these are sea surface salinity (SSS), nutrient concentration and mixed layer depth. The significance of these parameters on controlling the partial pressures depends on the biogeochemistry of the oceanic regions[9,12].

Remote sensing approach in partial pressure estimation

The key parameters governing the upper ocean biophysical processes are sea surface temperature (SST) and marine chlorophyll (Chl *a*) concentration, and their precise measurements can be done on global as well as regional scale for world oceans using satellite remote sensors. Therefore, efforts have been made worldwide to derive various biophysical parameters potentially affecting the CO_2 partial pressures from SST and Chl *a*. For example, seawater pCO_2 was estimated by eq. (5) using total alkalinity and dissolved inorganic carbon[6].

$$pCO_2w = g \times (2 \times DIC - TA) + h. \quad (5)$$

where pCO_2w is the partial pressure of CO_2 in water, DIC the dissolved inorganic carbon, TA the total alkalinity,

g and h are constants. TA was estimated by eq. (6) as a function of SST[13].

$$\mathrm{TA} = e \times \mathrm{SST} + f. \quad (6)$$

Nutrient concentration was calculated as given in eq. (7) from SST and Chl a[14].

$$N = \alpha \times \mathrm{SST} + \beta \times \mathrm{SST}^2 + \gamma \times \mathrm{Chl}\ a + \delta \times \mathrm{Chl}\ a^2 + \varepsilon. \quad (7)$$

Lee *et al.*[15] derived dissolved inorganic carbon using SST and nutrient concentration, as given in eq. (8).

$$\mathrm{DIC} = a \times \mathrm{SST} + b \times \mathrm{SST}^2 + c \times N + d, \quad (8)$$

where a, b, c, d, e, f, g, α, β, γ, δ and ε mentioned in eqs (5)–(8) are estimated constant parameters from least square method.

The eqs (5)–(8) were combined to develop a semi-empirical quadratic relation given in eq. (9) for deriving sea surface pCO_2 as a function of SST and chlorophyll concentration[10].

$$\mathrm{pCO_{2sw}} = A \times \mathrm{SST} + B \times \mathrm{SST}^2 + C \times \mathrm{Chl}\ a + D \times \mathrm{Chl}\ a^2 + E, \quad (9)$$

where A, B, C, D and E are constants estimated through least square procedure from pCO_2w, Chl a and SST measurements. Monthly averaged satellite data for SST and Chl a were obtained from OCTS (Ocean Colour and Temperature Sensor) on-board ADEOS (Advanced Earth Observation Satellite) platform to develop monthly pCO_2 maps for subarctic and subtropical oceanic regions.

Other studies that incorporated satellite data for pCO_2 determination include application of statistical regression techniques on SST data from NOAA (National Oceanic and Atmospheric Administartion) AVHRR (Advanced Very-High-Resolution Radiometer) and Chl a from SeaWiFS (Sea-Viewing Wide Field-of-View Sensor) by Sarma *et al.*[16] for the North Pacific Ocean; deriving partial pressure for northern South China Sea by Zhu *et al.*[17] using SST and Chl a retrieved from AVHRR and SeaWiFS respectively; mapping pCO_2 over Huanghai and Bohai Sea by Zui *et al.*[18] from Aqua MODIS (Moderate Resolution Imaging Spectroradiometer) SST and SeaWiFS Chl a; using SST from AMSR-E (Advanced Microwave Scanning Radiometer-Earth Observing System) on-board Aqua and Chl a from SeaWiFS and MODIS on-board Terra and Aqua by Liu and Xie[19] for calculation of partial pressure for global oceans; use of SST and Chl a from MODIS for Hooghly estuary by Padhy *et al.*[12] and that by Jang *et al.*[20] where Chl a, coloured dissolved organic matter (CDOM) and band reflectance from Geostationary Ocean Color Imager (GOCI) on-board COMS (Communication, Ocean and Meteorological Satellite) satellite were used over East Sea.

Techniques for pCO_2 estimation

Stephens *et al.*[21] developed sea-surface pCO_2 maps for the North Pacific by deriving statistical relationships between the ship-measured pCO_2 and SST, and applying them for the entire region using satellite-derived SST with a root mean square error of ±17 μatm. The derived relation is given in eq. (10)

$$\ln[\mathrm{pCO_2(10°C)}] = A + B \times \mathrm{SST} + C \times \mathrm{SST}^2 + D \times \mathrm{longitude}. \quad (10)$$

Seasonal and inter-annual relationships between the CO_2 fugacity and SST from ship measurements were derived by Cosca *et al.*[22] for the central and eastern equatorial Pacific Ocean for El-Niño cool and warm event and non-El-Niño cool and warm event periods. The RMS values were ±20.3 and ±16.6 μatm for El-Niño warm and cool seasons respectively; ±28.8 and ±30.2 μatm for non-El-Niño warm and cool seasons respectively. The linear statistical algorithm obtained is represented in eq. (11)

$$\mathrm{fCO_2} = A + B \times \mathrm{SST}. \quad (11)$$

The seawater CO_2 partial pressures in the North Pacific Ocean were derived from ship measurements of Chl a and SST[10] and pCO_2 maps for the region were developed using satellite-derived Chl a and SST. The RMS value for the satellite-derived pCO_2 was ±21 μatm. The incorporation of Chl a along with SST in the pCO_2 derivation reduced the RMS error compared to the previous study by Stephens *et al.*[21], who developed pCO_2 maps from SST data in this region. The algorithm developed by Ono *et al.*[10] for sea-surface pCO_2 is given in eq. (9).

Distribution of sea-surface pCO_2 in the North Pacific Ocean was mapped by Sarma *et al.*[16] from satellite-derived Chl a, SST and SSS applying multiple regression equations developed from *in situ* data. The RMS error obtained for the satellite-derived pCO_2 was 17–23 μatm. The algorithms were developed for spring and summer periods, and the general form of the algorithm is given in eq. (12)

$$\mathrm{pCO_2} = A - B \times \mathrm{SST} + C \times \mathrm{SSS} - D \times \mathrm{Chl}\ a. \quad (12)$$

Zhu *et al.*[17] estimated the sea-surface CO_2 partial pressures and CO_2 fluxes in the northern South China Sea using statistical relationship derived from *in situ* measurements of SST and Chl a and pCO_2 maps were developed from the satellite-derived SST and chlorophyll. Two algorithms were developed using regression analysis for deriving sea-surface pCO_2, the first with *in situ* SST data, and

the other with *in situ* SST and chlorophyll measurements. The satellite-derived pCO_2 was compared with the *in situ* values, which showed an RMS error of 4.6 μatm for the two-parameter algorithm, while it was found to be 25.1 μatm for the SST-based relation.

Relationship of pCO_2 and SST is given in eq. (13)

$$pCO_2 = A \times SST^2 - B \times SST + C. \quad (13)$$

Equation (14) showing the pCO_2 relationship with SST and Chl *a*

$$pCO_2 = A \times SST^2 + B \times Chl\ a^2 - C \times SST - D \times Chl\ a + E. \quad (14)$$

Ship-board measurements of pCO_{2sw}, SST and salinity were used to develop the partial pressure algorithm for seawater from SST, salinity and time component by Takamura *et al.*[23] over the eastern and western North Pacific Ocean. The time parameter was introduced to address the temporal variations. The relation can be expressed as follows

$$pCO_{2sw} = a0 + a1 \times SST + a2 \times SSS + a3 \times t, \quad (15)$$

where t is the time elapsed (months), and maximum significance among the parameters on the variability of partial pressure is exhibited by SSS. The RMS error obtained for the eastern North Pacific Ocean was ±11.3 μatm. For the western region, separate temperature conditions were considered for statistical analysis, where the error obtained was ±13.4 μatm for <17.5°C and ±12.1 μatm for ≥17.5°C.

Zui *et al.*[18] studied the seasonal variability of seawater pCO_2 in the Huanghai and Bohai Sea in relation to SST and Chl *a* using ship measurements. The study proposed an empirical relation between pCO_2, SST and Chl *a* to develop pCO_2 maps using satellite data. The satellite-derived pCO_2 value showed an RMS error of 13.45 μatm. The algorithm was developed for three different SST ranges, viz. SST < 12°C, 12°C ≤ SST ≥ 23°C, and SST > 23°C. The basic form of the algorithm can be written as follows

$$pCO_2 = A \times SST + B \times SST^2 - C \times Chl\ a + D \times Chl\ a^2 + E(T). \quad (16)$$

Carbon dioxide fugacity in the East Sea was derived from *in situ* measurements of dissolved organic matter, SST, salinity, mixed layer depth (MLD), Chl *a* and band reflectance[20]. The fCO_2 was derived using multivariate nonlinear regression (MNR), where SST showed maximum correlation with pCO_2 distribution and the major contributing factors for fCO_2 variations were SST, salinity and MLD. The MNR algorithm is represented in eq. (17).

$$fCO_2 = \sum_{i=1}^{n} k_i x_i + \sum_{l=1}^{n-1} \sum_{m=l+1}^{n} k_{lm} x_l x_m + \sum_{j=1}^{n} k_j x_j^2, \quad (17)$$

where n is the number of input parameters, x_i each input parameter and k is the coefficient associated with each term. The RMSE obtained for validation of the algorithm was 10.59 μatm.

Seawater pCO_2, SST and SSS time-series data for the Bay of Bengal (BoB) open ocean waters have been used to derive multiple linear regression models[24]. The empirical relation obtained was applied on satellite SST and SSS to develop the pCO_2 map for the case 1 waters of BoB. The relation is given in eq. (18)

$$pCO_2 = 11.81\ SST + 11.71\ SSS - 337.1, \quad (18)$$

where RMSE for the validation of the derived pCO_2 was 9.22 μatm.

Air–sea CO_2 fluxes distribution – case studies

Assessment of the spatial and temporal distribution of CO_2 fluxes is important in understanding the efficiency of the ocean to control excess quantities of CO_2 gas released into the atmosphere and balancing the atmospheric CO_2 concentration. The capacity of the oceans to act as the anthropogenic CO_2 sink will be reduced eventually, upsetting the seawater carbonate speciation and the marine carbon cycle. The quantification and analysis of CO_2 fluxes between ocean and atmosphere will provide information regarding the past and current trends in CO_2 gas regulation by the oceans[25,26].

Indian Ocean

A study on CO_2 emissions over the Arabian Sea (AS) showed a supersaturation of pCO_2 during the southwest (SW) monsoon leading to strong outflux to the atmosphere[27]. Extreme supersaturation levels reaching up to 750 μatm were found along the Omani coast and high pCO_2 values of around 525 μatm along with cold upwelled waters were observed about 300 NM (nautical miles) off the coast due to Ekman pumping. Variations in the flux densities were evident from the coastal region towards the open ocean with values ranging from 43,435 mmol m^{-2} yr^{-1} in the coast to 730 mmol m^{-2} yr^{-1} in the open-ocean waters. The SW monsoon has a significant role in the annual CO_2 emissions to the atmosphere with total emissions ranging from 0.672 to 1.73×10^{15} mmol C. The wind forcing in combination with intense coastal upwelling during this season makes the Arabian Sea a major CO_2 source.

Analysis of temporal variations in CO_2 partial pressures and CO_2 fluxes over the Arabian Sea was done by Goet *et al.*[28] using continuous pCO_2 measurements of seawater and atmosphere for the year 1995. Strong physical forcing due to the seasonal monsoons plays a major role in regulating the Arabian Sea partial pressures. Variations in pCO_2 were found to be very small in the offshore

regions with values less than 40 μatm while that of coastal areas crossed around 260 μatm. The monthly and annual fluxes were calculated using SST, wind speed and pCO_2 data. The mean monthly values ranged from 99.6 to 528 mmol m^{-2} yr^{-1} for most of the year, while they showed significantly higher values during the SW monsoon with values reaching up to 3753.6 mmol m^{-2} yr^{-1} along the coast of Oman resulting from the strong upwelling. The Arabian Sea was found to act as an annual CO_2 source to the atmosphere with annual emissions of 0.159×10^{15} mmol C yr^{-1}.

Sarma *et al.*[29] analysed the seasonal and interannual variations in pCO_2 and total CO_2 (TCO_2) in the central and eastern Arabian Sea. The total CO_2 was determined by coulometric methods, and pCO_2 was computed from TCO_2 and pH. Seasonal changes in the TCO_2 were observed with variations in ocean circulation and primary production. TCO_2 values were found high during winter and low in the SW monsoon season. This was attributed to the winter convective mixing bringing subsurface CO_2 to the upper ocean and accelerated primary production during SW monsoon resulting from nutrient enrichment. Seawater pCO_2 was higher in all the seasons compared to the atmosphere in the Arabian Sea, except during the SW monsoon on the Indian coast. The analysis revealed that the Arabian Sea acts as a perennial CO_2 source during almost all seasons with annual emissions of 1.02×10^{15} mmol C yr^{-1} to the atmosphere.

Data collected during the Indian and US JGOFS programme, and Indian Land–Ocean Interactions in the Coastal Zone process study program were used to analyse the sea-surface pCO_2 and air–sea CO_2 fluxes[30]. Dissolved inorganic carbon content was derived from SST, salinity and chlorophyll using multiple linear regression. Total alkalinity from salinity and surface pCO_2 from carbonate dissociation constants were computed. High variability was observed in the seasonal and spatial partial pressure distributions and CO_2 fluxes in the Arabian Sea. A rise in the partial pressures was observed on the western coast during the SW monsoon induced by the intense upwelling. The highest surface partial pressure values were observed during the SW monsoon with about 700 μatm in the upwelling region of the western coast and >480 μatm along the SW coast of India. In the open ocean, high partial pressures were found in the northern Arabian Sea with values >420 μatm. An increase in the SST by 2°–3°C was observed in the fall monsoon compared to the SW monsoon. This resulted in a decrease in surface pCO_2 levels to 360–380 μatm in the western coastal regions, particularly the Arabian coast due to stratification and biological processes triggered by high nutrient availability and subsequent elevated chlorophyll content. A lowered partial pressure range 370–380 μatm was noticed in the central Arabian Sea owing to the increase in SST and increased bacterial respiration. Lower pCO_2 values were found along the SW coast of India during the northeast (NE) monsoon resulting from the inflow of low-saline waters from the BoB. The decrease in partial pressures caused a lowering of the coastal pCO_2 values to <360 μatm, while the central Arabian Sea showed a partial pressure range 380–420 μatm. The spring intermonsoon was characterized by increased coastal partial pressures from <360 μatm to about 370–380 μatm, resulting from the reversed surface circulation breaking off the influence of low-saline water mass. Analysis of the CO_2 flux distribution showed stronger emissions from the western coast and the annual emissions from the Arabian Sea were about 2.04×10^{15} mmol C yr^{-1}, thereby acting as a CO_2 source.

A study carried out in 27 estuaries along the Indian coast by Sarma *et al.*[31] reported that the CO_2 emissions were 4–5 times higher in the monsoon season than the dry period. The pCO_2 values ranged from 300 to 18,492 μatm. The monsoonal fluxes were about 0.0363×10^{15} mmol C, while the annual CO_2 emissions from the estuaries were 0.0436×10^{15} mmol C yr^{-1}. The high fluxes during the wet period are attributed to the high organic matter content in the estuaries due to the monsoonal river discharge and subsequently increased rates of microbial aerobic respiration. The occurrence of phytoplankton blooms drawing down the CO_2 levels and the increase in light penetration with decreased suspended sediment concentration in summer account for the reduced summer fluxes.

Observations on the western continental shelf of BoB by Sarma *et al.*[32] showed that the sources and sinks of CO_2 in the shelf region are dependent on the river discharges and the distribution of the discharged water by the East India Coastal Current (EICC). The CO_2 partial pressures in SW coast are regulated by the peninsular river discharge and in NW region by the Ganges river discharge. The partial pressures were found to be lower than that of the atmospheric levels in the NW region, whereas the SW coast exhibited supersaturation. The lower values in the NW region were caused by the comparatively low salinity due to freshwater discharge and higher productivity than the SW coast. The CO_2 fluxes for the SW region were 2847 mmol m^{-2} yr^{-1}, thus acting as a CO_2 source and for the NW region were –3978.5 mmol m^{-2} yr^{-1}, thereby acting as a sink. The mean fluxes for the entire western coast were about 73 mmol m^{-2} yr^{-1}, which suggests that the coast acts as a net annual source.

A study of the atmospheric CO_2 sinks in the southern Indian Ocean by Valsala *et al.*[33] examined the seasonal, interannual and interdecadal variability of the CO_2 fluxes. They reported that the southern tropical-to-subtropical Indian Ocean region is a broad zone of subduction, where the subducting water mass traps and carries atmospheric trace gases from the atmosphere. Highest concentration of anthropogenic CO_2 was found to be at 150 m depth between 15°S and 50°S. The study area was divided into two distinct zones, namely north and south located at

15°–35°S and 35°–50°S respectively. In the north zone the CO_2 flux was found to be controlled by the solubility pump, while CO_2 uptake was dominated by solubility as well as a biological pump in the south zone due to the high phytoplankton concentration in the south. Analysis of wind stress over this region indicated a coincidence of the locations of the largest concentration of anthropogenic CO_2 with the subtropical zone of positive wind stress curl. Since a positive curl indicates the Ekman downwelling process in the southern hemisphere, the subsurface CO_2 trapping in the southern Indian Ocean was reported to be induced by atmospheric forcing due to the presence of positive wind stress. The study concludes that the deepening of subduction and consequent invasion of CO_2 gas into the northern part of the Indian Ocean has resulted in the sinking of anthropogenic CO_2 in this region.

The CO_2 fluxes over the Indian Ocean from 1990 to 2009 were estimated by Sarma *et al.*[34] as part of the Regional Carbon Cycle Assessment and Process (RECCAP). The fluxes in the northern Indian Ocean (18°S–30°N) were regulated by the solubility pump, while both the biological and solubility pumps equally dominated the southern region (44°–18°S). The results suggested that the southern Indian Ocean acts as a net annual CO_2 sink with flux value -9.77×10^{15} mmol C yr^{-1} and the northern counterpart acts as a net source with annual mean value 2.95×10^{15} mmol C yr^{-1}. The entire Indian Ocean acts as a net sink for atmospheric CO_2 with annual flux value -8.41×10^{15} mmol C yr^{-1}. The monsoonal wind action and upwelling processes in the northern Indian Ocean contribute to CO_2 release, whereas the low saline waters in the southern region enhance CO_2 uptake.

Seasonal and interannual variability study of the CO_2 flux by Valsala and Maksyutov[35] simulated CO_2 flux over the northern Indian Ocean by coupling the biogeochemical model with an ocean tracer transport model which is based on 30-year reanalysis ocean data such as ocean currents, temperature and salinity. Maximum variability was observed in the coastal AS and southern Peninsular India (SP). The modelled CO_2 flux values showed an annual emission scenario of $(2.72 \pm 0.909) \times 10^{15}$ mmol C yr^{-1}. The CO_2 flux anomalies in AS and SP were then correlated with two major climate anomalies, i.e. ENSO (El Niño-Southern Oscillation) and Indian Ocean Dipole/Zonal Mode (IODZM). It was observed that a strong correlation of CO_2 flux in AS and SP with IODZM is accompanied by a weak correlation of the flux with ENSO and vice versa. The surface-water pCO_2 was calculated from dissolved inorganic carbon (DIC), temperature, alkalinity and salinity. Analysis of the effects of these components on the flux showed an increase in the temperature effect with a positive correlation between the flux and IODZM and vice versa in AS, whereas the CO_2 emission in SP was mainly controlled by changes in DIC. The DIC effect in SP was found to weaken during a negative correlation between CO_2 emission and ENSO.

Time-series estimation of chemical processes in the upper 100 m water column was carried out in the Visakhapatnam region on the western coast of BoB[36]. Measurements were made for temperature, salinity, DIC, TA and nutrients to derive the seawater pCO_2 and the atmospheric pCO_2 was measured directly using a pCO_2 sensor. The seawater pCO_2 values showed an increasing trend with a depth ranging from 450 μatm at the surface to 1300 μatm at 100 m depth. The CO_2 fluxes were estimated empirically from the CO_2 solubility, gas-transfer velocity and partial-pressure difference between air and seawater. The calculated fluxes suggest that the region acts as a net CO_2 source to the atmosphere with average values of 0.186 mmol C m^{-2} yr^{-1}. The strong wind mixing of the sea-surface water was found to be a significant contributing factor for the fluxes in this region.

Valsala and Murtugudde[37] analysed the intraseasonal and mesoscale variations occurring in the CO_2 gas transfer during boreal summer (June–September) over the western Arabian Sea. The oceanic circulation triggered by the fluctuations in the atmospheric circulation in this season induces intense upwelling, eddy formation, increased salinity levels and consequently elevated levels of nutrients and carbon content in the surface waters of the Somali coast. The study used a biogeochemical model called Ocean Tracer Transport Model (OTTM) based on reanalysis ocean data and surface fluxes. The sea-surface pCO_2 was observed to undergo consistent intraseasonal variability in this region driven by the changes in SST and DIC content. The analysis showed a correlation of 0.86 between pCO_2 variability and temperature, which was found to decrease with increased upwelling and Ekman pumping. The pCO_2 variability during the boreal summer accounts for 40% of the mean monthly CO_2 flux variability in this season. The seasonal co-variability of the outflux of CO_2 gas with decreased SST can be explained by the increase in DIC resulting from intense upwelling. The study also establishes the significance of ocean dynamics in the pCO_2 and CO_2 flux intraseasonal variability by analysing the response of SST, DIC, alkalinity, pCO_2 and biological pumps to the dynamic processes in the ocean system.

A CO_2 flux pattern study between seawater and air over the southern BoB reported high seasonal variations in the physico-chemical and biological parameters[38]. The summer season was characterized by intense light penetration due to low cloud cover, reduced nutrient concentration due to the absence of river discharge and vertical mixing, consequent decrease in biological production, lowering of surface pCO_2 and negative CO_2 fluxes. The summer trends in the physical, chemical and biological factors reversed during the monsoon season with strong wind action and enhanced upwelling contributing to high pCO_2 values and sea-to-air fluxes. The annual CO_2 flux variability ranged from –1752 to 4088 mmol C m^{-2} yr^{-1} with an annual mean of 73 mmol C m^{-2} yr^{-1}.

CO_2 partial pressure and flux measurements were made in the Hooghly estuary by Padhy *et al.*[12] using *in situ* measurements and satellite data. SST and Chl *a* were used to derive the seawater partial pressure which revealed supersaturation levels. The high riverine fluxes account for high DIC levels in this region, contributing to enhanced pCO_2 levels. The winter pCO_2 levels ranged from 340 to 375 μatm and summer values were found to be about 450 μatm. The comparatively lower values in winter are attributed to the lowering of salinity by the river discharge and weak wind action. The average annual CO_2 fluxes were about 4.5×10^4 mmol C m^{-2} yr^{-1}, proving the region as a CO_2 source.

Pacific Ocean

Midorikawa *et al.*[39] analysed the CO_2 partial pressure distribution and concentration of DIC and nutrients in the western subarctic North Pacific region. The fluxes derived during winter to summer were about 5840 mmol m^{-2} yr^{-1}, and during summer to autumn about –1460 mmol m^{-2} yr^{-1}. The high fluxes during the winter to summer season is due to high DIC in the mixed layer and deep vertical mixing. The decreased CO_2 partial pressures due to increased biological consumption and the comparatively low wind speed during summer season have resulted in the reversal of fluxes during the summer to the autumn period.

CO_2 fugacity measurements of surface water were carried out by Feely *et al.*[40] in the equatorial Pacific Ocean, which showed a CO_2 supersaturation of seawater with average value of 473 μatm. The higher partial pressure values were attributed to enhanced upwelling in the region which resulted in about 20–40 μatm higher than normal values with the highest values obtained in the southern equatorial Pacific, where the upwelling was intense. The drawdown of CO_2 by the primary productivity of the ocean was counterbalanced by upwelling and surface warming, thus maintaining the sea-to-air fluxes. A relationship between the CO_2 gas transfer and wind speed was developed along with estimates of air–sea partial pressure differences to derive CO_2 fluxes. The average CO_2 flux was 3.7×10^3 mmol m^{-2} yr^{-1}. The variability in fluxes was contributed mainly by the partial pressure changes in this region, where the influence of wind field and gas transfer variability was found to be less.

Interannual and decadal flux variability over the equatorial Pacific Ocean was studied by Feely *et al.*[41] using ship measurements of SST and CO_2 fugacity collected during the period November 1981 to June 2004, which included five El Niño and four La Nina events. An increase in the sea-surface CO_2 was observed at a similar rate to that of atmospheric CO_2, indicating an active exchange of air–sea CO_2 in the equatorial waters. A major inter-annual ENSO variability was observed for the entire region from the analysis of seawater fugacity in combination with SST and wind data, while seasonal changes were noted to be weak in the eastern Pacific. A prominent increase in fCO_{2sw} (CO_2 fugacity of seawater) was observed over the entire study period and a slight intensification of the CO_2 outflux after the 1997–1998 warm-to-cold regime shift resulting from the Pacific Decadal Oscillation (PDO).

Ship measurements of SST, salinity, sea surface and atmospheric CO_2 from the NW and northeast Pacific were analysed by Takamura *et al.*[23] to study the interannual and seasonal variability in the CO_2 fluxes from 1999 to 2006. In both western and eastern North Pacific, the fluxes showed minimum values during late summer (August/September) and reached a maximum during late winter (January/February). The summer flux values over the western region ranged from –73 to 219 mmol m^{-2} yr^{-1}, where the flux maximum during the winter exhibited a range 2993–4161 mmol m^{-2} yr^{-1}. The eastern region had the minimum flux range within –1058.5 to –657 mmol m^{-2} yr^{-1} during summer and maximum range 1898 to 2482 mmol m^{-2} yr^{-1} in winter. The fluxes from air to seawater were found to increase over the period of study where the western North Pacific showed a comparatively higher rate of 69 ± 18.25 mmol m^{-2} yr^{-1}, indicating a much stronger CO_2 sink than the eastern region with a flux rate of 32.85 ± 10.95 mmol m^{-2} yr^{-1}.

Climatic impacts on the CO_2 flux variability in the northern Pacific Ocean were studied by Valsala *et al.*[42] for the period 1980–2004. CO_2 flux data were analysed for spatio-temporal variability over the study area, followed by a comparative analysis of interannual variability with the seasonal changes. Spatial flux variability induced by PDO, generated by the SST anomalies in the North Pacific, was analysed using correlation analysis between monthly anomalies of CO_2 fluxes and PDO index. The analysis revealed small spatial variability of fluxes in relation to PDO, which was attributed to the weak interannual flux anomalies in the North Pacific. Flux anomalies were noticed in the subtropical gyre, where PDO-accompanied SST cooling had resulted in CO_2 absorption and eventual generation of the sink, thus establishing an active flux response to climate variability. It was observed that thermocline shifts associated with PDO were reflected in subsurface DIC levels.

Valsala *et al.*[43] studied the seawater pCO_2 and CO_2 fluxes over the equatorial Pacific for seasonal, interannual and multi-decadal variability for the period 1961–2005. They used the biogeochemical model based on the reanalysis ocean products to study the seasonal cycle and spatio-temporal characteristics of the pCO_2 and CO_2 fluxes during the ENSO period, both individual and combined effects of the wind and ocean dynamics on the variability of pCO_2 and CO_2 fluxes, effect of the canonical and Modoki ENSOs on the fluxes and also the carbon dynamics variability and its association with PDO. The analysis revealed a dominance of ENSO on the interannual flux

variability. A reduction in CO_2 emission was observed in the central to eastern equatorial Pacific during the El Niño period. The effect of canonical El Niño was found mainly between 160°W and 110°W, while the El Niño-Modoki dominated over the western (160°E–160°W) and far eastern (110°–90°W) equatorial Pacific. A correlation of pCO_2 was observed with the canonical El Niño to the east of 140°W and with the El Niño-Modoki to the west of 140°W. A nonlinear relationship between the pCO_2 and CO_2 fluxes was introduced in some parts of the equatorial Pacific by individual as well as combined influence of the ENSO-induced wind and ocean dynamics. Abrupt shifts were observed in the equatorial Pacific CO_2 sinks during the 45-yr study period. The multi-decadal variability caused an increased uptake of atmospheric CO_2 from 1961 to 1982, followed by a reduction until 2000 and again a strengthening of the sinking process thereafter. The study concluded that PDO and El Niño-Modoki are the major controlling factors of the pCO_2 and CO_2 flux multi-decadal variability, while the interannual variability is dominated by the canonical El Niño events.

Time-series data of high-resolution CO_2 flux were obtained by Sutton *et al.*[44] over the Pacific Ocean from moored observations of sea-surface pCO_2 and wind speed measurements. These moorings are situated in four specific locations of north and south subtropical oligotrophic region, subtropical and subarctic North Pacific regions. Atmospheric and seawater pCO_2, SST and salinity were measured from four locations using a moored autonomous pCO_2 system set-up in open-ocean buoys located in the subtropical North and South Pacific and subarctic North Pacific regions. Total alkalinity was calculated using SST and salinity, which was further used along with the seawater pCO_2 to calculate DIC. The CO_2 flux was calculated using gas transfer velocity, CO_2 solubility and pCO_2 difference between seawater and atmosphere. The analysis showed an eventual shift of this oceanic region from an annual sink to a source of CO_2, which was attributed to elevated levels of sea-surface pCO_2 resulting from thermal anomalies in the North Pacific region. The subtropical North Pacific location proved as the strongest sink with –647.7 mmol C m^{-2} yr^{-1} and the southern subtropical oligotrophic region was the only source with 106.8 mmol C m^{-2} yr^{-1}.

Atlantic Ocean

Interannual CO_2 flux variability over the northern North Atlantic Sea for the period 1981–2001 during winter season was analysed by Olsen *et al.*[45]. The data analysis was carried out from October to March for calculating the fluxes using seawater CO_2 fugacity, CO_2 mole fraction, gridded datasets of SST, sea-level pressure and wind speed. A net annual air-to-sea CO_2 flux of 1.818×10^{15} mmol was obtained for the winter season for the study period with an interannual variability of ±0.7%. This variability was attributed mainly to the variations in wind speed and atmospheric CO_2 fugacity. The air–sea CO_2 flux was also found to be sensitive towards the variations in the North Atlantic Oscillation (NAO) and an increased CO_2 influx to the ocean with an increase in NAO index was observed.

A study on the interannual variability in the CO_2 sinks in the North Atlantic subtropical gyre over a two decadal period was carried out by Bates[46]. Oceanic CO_2 was monitored continuously from 1983 to 2005, which showed an annual increasing trend in DIC and pCO_2 with an increase in atmospheric CO_2 concentration, followed by a subsequent decrease in seawater pH, carbonate concentration and $CaCO_3$ saturation states. An imbalance in the seasonal CO_2 sink and source rates was also observed attributed to the comparatively higher CO_2 uptake in winter than the summer outflux, proving this region as a CO_2 sink. The net air–sea CO_2 flux was estimated to be in the range –815 to –1295 mmol C m^{-2} yr^{-1}. The occurrence of hurricane events enhanced the fluxes during summer season. The fluxes also exhibited a correlation with NAO variability in the summer and fall seasons. However, poor correlations were found in the case of the winter fluxes with NAO or Arctic Oscillation (AO), whereas they showed higher values during the El-Niño years. An increase of 5–17% in the net annual CO_2 flux rate was also observed during the study period.

Oliveiraa *et al.*[47] carried out a study on the CO_2 fluxes over coastal and open-ocean waters of the southern Atlantic Ocean during the austral winter period of 2015. They analysed the eddy covariance measured *in situ* CO_2 fluxes for 13 and 14 July 2015 in three sub-regions of the study area, namely the Brazilian southeast coastal region (BCR), the region influenced by the Brazil current (BC) and the open ocean (OPO). The results showed a contrasting flux trend over the three selected study regions. The BC and BCR regions were found to act as a carbon sink, as shown by the measured negative flux values from these regions. It was noticed that an intensified mixing process at the ocean–atmosphere interface in the BC region induced by intense winds in this oceanic part favoured CO_2 absorption by the ocean waters, which was again strengthened by the temperature difference between the sea surface and atmosphere at the marine–atmospheric boundary layer (MABL). The presence of coastal upwelling was found to be the consequence of CO_2 sinking in the BCR region. Here the low values of SST and SSS were observed to increase the CO_2 solubility of surface waters, resulting in enhanced primary productivity. In contrast to BC and BCR, the OPO region lacks the CO_2 sink as a result of the decreased sea level pressure and weakened wind speeds triggering vertical movements in the MABL over this area leading to a decrease in atmospheric CO_2. As a result, the OPO region acts as a CO_2 source to the atmosphere. The study region exhibited a

mean sinking behaviour in the flux trends during the sampling period caused by the combined impact of large-scale atmospheric processes and local atmospheric modulations due to SST variations. The authors suggested the inclusion of further *in situ* data with better spatial and temporal resolution for enhanced understanding of the carbon budget over the southwest Atlantic region[47].

Orselli *et al.*[48] studied the significance of the Agulhas eddies in the air–sea CO_2 fluxes over the south Atlantic Ocean using *in situ* measurements from six eddies and their surrounding waters carried out as a part of the FORSA (Following Ocean Rings in the South Atlantic) cruise during 27 June to 15 July 2015. The study area was divided into the eastern and western basins, with the Mid-Atlantic Ridge acting as the boundary. The sea surface and atmospheric CO_2 partial pressures were calculated from the measured parameters like temperature, salinity and CO_2 mole fraction for both seawater and overlying air. The surface temperature, salinity and seawater CO_2 partial pressure values were comparatively less in the eastern basin, while low values of atmospheric partial pressures were obtained in the western basin. Eastern basin fluxes were observed to be regulated by physical forcing mechanisms driven by the Agulhas eddies, whereas biological dominance could be considered in the case of flux trends in the western basin. The difference in the ocean and atmospheric partial pressures was calculated to be –39.1 μatm, proving the oceanic region to be a sink for atmospheric CO_2 with a mean flux value of –1372.4 mmol m^{-2} yr^{-1}. Temperature domination in CO_2 absorption was observed during the study period and the contribution of Agulhas eddy in this CO_2 uptake was found to be -262×10^5 mmol C yr^{-1}.

Studies over other oceanic regions

The study of seasonal variations in CO_2 and nutrients in the high-latitude oceanic regions by Takahashi *et al.*[25] examined the CO_2 and nutrient concentration, and pCO_2 data to define their seasonal relationship and compare the inter-ocean variations of these parameters. The spring-time phytoplankton blooms in the North Atlantic Ocean were found to reduce the surface pCO_2, nutrient and CO_2 concentrations which lasted only until the exhaustion of the available nutrients. Such processes were limited only to the high-latitude waters north of 40°N. In the North Pacific, the seasonal variations in the CO_2 and nutrient concentrations occurred as a gradual process, while a partial consumption of nutrients was observed in the subarctic North Pacific and the Southern Ocean regions. The concentration of CO_2 and nutrients and the surface pCO_2 showed higher values during winter in the subpolar and polar waters of South Atlantic, North Pacific, North and South Atlantic Oceans compared to the summer season. The high-latitude areas of North Atlantic, North Pacific and Weddel Sea acted as sources of CO_2 to the atmosphere in winter and sinks in summer. This seasonality in the fluxes was attributed to intense winter upwelling and increased summertime photosynthesis. However, in the case of tropical waters, CO_2 uptake from the atmosphere was found to occur during winter while outfluxes were observed in summer. Here, temperature was the key element regulating the seasonal pCO_2 fluctuations due to weakening of biological factors. The combined effect of subtropical cooling and strong photosynthetic consumption of CO_2 in the subpolar waters resulted in the generation of an intense sink in the subtropical convergence region.

Estimation of global CO_2 fluxes by Takahashi *et al.*[49] involved the measurement of partial pressure differences between air and ocean surface for around 250,000 global observations. Distribution of global monthly pCO_2 differences was constructed from the lateral advection–diffusion transport equation, and the net CO_2 flux was calculated from the partial pressure and CO_2 gas transfer coefficients. An annual net uptake of $13.6–30.45 \times 10^{15}$ mmol C yr^{-1} by the oceans was estimated, and the analysis revealed the temperate and polar regions as CO_2 sinks while equatorial region as the source. The Atlantic Ocean was found to be the most intense sink, accounting for about 60% of the global CO_2 uptake. The Pacific equatorial belt was a strong CO_2 source which was balanced by the temperate sinks; thus the Pacific Ocean was observed to be neutral in terms of flux. The contribution from both the Indian Ocean and Southern Ocean combined for the CO_2 uptake was 20%.

Climatological monthly pCO_2 data, seasonal effects of biological factors and temperature were used by Takahashi *et al.*[9] to calculate the global air–sea CO_2 fluxes, where the monthly and annual fluxes were estimated using mean monthly wind-speed data. The net annual uptake estimates were obtained as 50×10^{15} mmol C yr^{-1} and the regions between 40° and 60° lat. were found to be the major CO_2 sinks in both hemispheres consequent to the mixing of nutrient-rich subpolar cold waters with the poleward-flowing warm waters along with the biological CO_2 uptake, subsequently resulting in decreased pCO_2 in the subpolar waters. The high wind speed over the low-surface pCO_2 waters also enhanced the oceanic CO_2 uptake. Thermal and biological effects were observed to control the pCO_2 seasonality for specific areas, whereas pCO_2 seasonal maximum was regulated by thermal and physical forcing such as upwelling. The biological component dominated in the eastern equatorial Pacific, equatorial and subpolar waters, the northwestern Arabian Sea, Antarctic and the sub-Arctic North Pacific coastal waters, while the temperature component was found to influence the subtropical gyre areas.

Air–sea CO_2 fluxes over the northern South China Sea were derived by Zhai *et al.*[50] during spring, summer and autumn seasons. Data collection for temperature, pCO_2,

and salinity was done during the ship measurements conducted for the summer of 2000, spring of 2001 and fall season of 2002. The surface-water partial pressures in the offshore region of about >100 km from the coast were found to be in the range 360–450 μatm, and were higher than that of the atmosphere in all three seasons. The sea-to-air difference in the partial pressures was observed to be about 0–50 μatm in the spring season, 0–90 μatm in autumn and 50–100 μatm in the summer season. The average flux values from the ocean to the atmosphere were 2555 mmol m^{-2} yr^{-1} for summer and in the range 365–1095 mmol m^{-2} yr^{-1} during spring and fall seasons. These observations reveal that the seasonal variations in sea surface partial pressures are influenced primarily by temperature changes and the region acts as a net CO_2 source.

McNeil *et al.*[51] carried out a study in the Southern Ocean to empirically derived the seawater CO_2 partial pressures from SST, SSS, DIC and TA and computed the CO_2 fluxes for winter and summer seasons. The CO_2 partial pressures were higher up to 40 μatm in winter than in summer in the Antarctic Zone due to winter upwelling. In the Sub-Antarctic Zone, winter cooling decreased the pCO_2 values by up to 70 μatm. The changes in winter to summer DIC showed significant variations in pCO_2. The high DIC values in winter due to upwelling enhanced pCO_2 by up to 150 μatm in the Antarctic Zone, while in the Sub-Arctic Zone temperature-induced seasonal partial pressure changes dominated the DIC variations. The estimation of CO_2 fluxes showed that the Southern Ocean acts as a weak to moderate global sink with average flux values -9.09×10^{15} mmol C yr^{-1}.

The Southern Ocean is reported to act as a significant atmospheric CO_2 sink based on observational and modelled datasets. However, a study conducted by Gray *et al.*[52] based on flux measurements using biogeochemical profiling floats as a part of the Southern Ocean Carbon and Climate Observations and Modeling (SOCCOM) project during 2014–2017, reported a strong CO_2 source region around Antarctica resulted from upwelling of deep carbon-rich waters. The lack of ship-based observations in this high-latitude region can be the principal reason behind the delay in identifying this CO_2 source region. Datasets of various parameters like temperature, salinity, pH, NO_3 and dissolved oxygen from 35 profiling floats were analysed. The study area was divided into five zones based on SST, salinity and nutrient content, namely Subtropical Zone (STZ), Sub-Antarctic Zone (SAZ), Polar Frontal Zone (PFZ), Antarctic Southern Zone (ASZ) and Seasonal Ice Zone (SIZ) from north to south. The seasonal average of CO_2 fluxes was calculated for each zone, and the results were found to agree with the temperature and DIC-driven regulations in the summer CO_2 uptake by biological processes and winter release. The analysis showed that despite the outgassing in STZ and SAZ, these regions acted as sinks with flux values -7.95×10^{15} and -2.27×10^{15} mmol C yr^{-1} respectively. While PFZ and SIZ were found to act as weak sources with negligible outgassing (0.227×10^{15} mmol C yr^{-1}), ASZ was a substantial CO_2 source, outgassing 8.18×10^{15} mmol C yr^{-1}.

Mongwe *et al.*[53] examined the significance of temperature and DIC in driving the seasonal cycle of CO_2 flux in the Southern Ocean. According to recent studies, the seasonality in CO_2 fluxes over this oceanic region is not well simulated by the Coupled Model Inter-comparison Project version 5 (CMIP5) as evident from a comparison with observational data. This study explains the bias in the CMIP5 model related to seasonal variations in SST and DIC. SST-related biases were grouped as group-SST, the most commonly observed bias, exhibiting an exaggerated rate of seasonal temperature variations during warming and cooling peaks in the spring and autumn seasons. Group-DIC bias showed exaggerated primary production scenarios, indicating a DIC-dominated flux variation. The study selected 10 CMIP5 models for analysis, based on the availability of the required parameters like pCO_2, CO_2 fluxes, SST, vertical temperature fields, surface DIC, annual DIC, mixed layer depth (MLD), surface oxygen, chlorophyll and net primary production (NPP). The analysis showed a low model sensitivity for the inter-basin CO_2 flux differences. The study reports that this is most likely due to the low sensitivity of the carbon cycle in these models compared to the observational data, towards the inter-basin difference in the driver parameters of the fluxes. This results in a zonal uniformity in the seasonal flux biases. Moreover, since the flux direction is dependent on the air–sea partial pressure difference and the sea-surface partial pressures are regulated by the SST and DIC concentrations, the ability of the model to simulate the flux seasonality is dependent on the sensitivity of the model towards the regulation of fluxes by variations in SST and DIC. As the CMIP5 models lack proper representation of inter-basin contrasts in the CO_2 fluxes and phytoplankton biomass compared to observational and remote sensing data, the study concludes with remarks explaining the need for further studies with the next-generation models such as CMIP6, giving a proper representation of carbon process parameterization and dynamics of the water column physics.

Dynamics and trends of air–sea CO_2 fluxes

The Indian Ocean, divided by the Indian peninsula into western and eastern sub-basins, is a unique oceanic region for studying the CO_2 fluxes. The northwestern Indian Ocean observed a supersaturation of pCO_2 during SW monsoon leading to strong outflux to the atmosphere. This was found to be attributed to the monsoonal wind forcing and intense coastal upwelling in this region, where the Somalia and Omani coasts were identified as the peak upwelling regions[54]. The circulation, mixing and

advection of these upwelled waters to the eastern Indian Ocean are regulated by monsoon winds and eddy currents[55]. The Arabian Sea was found to act as an annual CO_2 source to the atmosphere and the maximum outflux recorded was 2.04×10^{15} mmol C yr^{-1} (ref. 30). The western Arabian Sea was observed to undergo rapid warming due to increasing SST according to the study conducted by Sreeush *et al.*[56], along with a decreasing trend in pH indicating acidification. The CO_2 sink and source regions in the northeastern Indian Ocean are regulated by river discharge and coastal currents. The river discharges in BoB were found to have a significant influence on the mixed layer and barrier layer processes[57,58]. Studies have reported upwelling regions triggered by strong monsoon winds around the Sri Lankan coast during summer monsoon and in BoB during NW monsoon[59–61], while the intensification of alongshore winds during summer monsoon induced strong upwelling along the coasts of Java and Sumatra, according to a study by Susanto *et al.*[62]. While the upwelling processes enriched surface pCO_2 levels, the enhanced primary production due to increased surface nutrient levels due to upwelling was found to reduce pCO_2 in the sea east of Sri Lanka[63]. The spatial variability study of fluxes in the western BoB reported that the southwestern region acts as a source, whereas the northwestern part acted as a sink due to the freshwater-induced low surface salinity, and the entire western part was a net source. The western BoB was a CO_2 source resulting from strong wind action. The seasonality observations in the southern BoB fluxes showed that this region acts as a summer sink due to lack of vertical mixing and monsoonal source due to wind action and upwelling with a wide range from –1752 to 4088 mmol C m^{-2} yr^{-1}. A study on the Indian Ocean biophysical processes reported that the shallowing of thermocline by the climatological winds in the coastal areas and Ekman pumping in the open ocean enhances upwelling in the Arabian Sea, whereas BoB lacks a strong upwelling system[64]. The entire Indian Ocean was identified as a net annual CO_2 sink by Sarma *et al.*[34] with an annual inward flux of -8.41×10^{15} mmol C yr^{-1}. The emissions were observed to be 4–5 times higher in the monsoon season compared to the dry period in the Indian coastal estuaries. A study of the Hooghly estuary revealed that the region acts as a net source of CO_2 with comparatively lower flux values in summer due to lowering of surface salinity and weak winds.

Flux studies over the Pacific Ocean were carried out in the western subarctic North Pacific, equatorial Pacific, the northwest and northeast Pacific, subtropical North and South Pacific and subarctic North Pacific regions. Observations in the western subarctic North Pacific showed this region to be a CO_2 source during winter to summer, and as a sink during summer to autumn. The high sea-to-air fluxes were due to high DIC in the mixed layer, and the deep vertical mixing in winter and decreased sea-surface CO_2 partial pressures in summer resulted from the increased biological consumption and comparatively low wind speed. The equatorial Pacific Ocean showed a CO_2 supersaturation of seawater caused by enhanced upwelling in this region. Highest outflux values were obtained in the southern equatorial Pacific where the upwelling was intense thus counterbalancing the surface CO_2 consumption by the ocean primary productivity. Interannual and decadal flux variability studies over the equatorial Pacific Ocean revealed an active exchange of air–sea CO_2. The interannual ENSO variability was strong in the entire region, while the seasonal changes were weaker in the eastern Pacific. PDO was found to intensify the sea-to-air fluxes in the equatorial region, while SST cooling related to PDO in the subtropical gyre was observed to enhance CO_2 sinking. The western North Pacific showed a much stronger CO_2 sink with minimum values during late summer and maximum during late winter. The Pacific Ocean showed an eventual shift from an annual sink to a source resulting from elevated thermal anomalies in the North Pacific region. The western subarctic North Pacific showed the highest sea-to-air fluxes of 5840 mmol m^{-2} yr^{-1} during winter[39], while maximum absorption by the sea surface was observed in the subtropical North Pacific with a flux value of –647.7 mmol C m^{-2} yr^{-1} (ref. 44).

The air–sea CO_2 flux over the northern North Atlantic Sea during winter season showed sensitivity towards variations in NAO where the air-to-sea fluxes tended to be stronger with an increase in the NAO index. An imbalance in the seasonal CO_2 sink and source rates was also observed in the North Atlantic subtropical gyre, which was interpreted to be caused by the relatively higher winter CO_2 uptake rates by the sea surface compared to the summer outflux, establishing this region as a CO_2 sink of –815 to –1295 mmol C m^{-2} yr^{-1} (ref. 46). Hurricanes and NAO were also found to contribute to flux variability. South Atlantic Ocean showed contrasting trends in the fluxes between coastal and open ocean waters[47], while the coastal region influenced by BC as well as BCR acts as a CO_2 sink, the open ocean waters found to be releasing CO_2 gas. The South Atlantic Ocean acts as a net CO_2 sink with a mean flux value of –1372.4 mmol m^{-2} yr^{-1} (ref. 48).

The northern South China Sea was reported to be a CO_2 source during spring, summer and autumn seasons with a maximum value of 2555 mmol m^{-2} yr^{-1} in summer[50]. A temperature-induced seasonality was observed in the sea-surface partial pressures with the region acting as a net CO_2 source. The Southern Ocean is known to be weak-to-moderate global sink where a winter upwelling induced increase in CO_2 partial pressures is obtained in the Antarctic Zone, while winter cooling decreases the pCO_2 values in the Sub Antarctic Zone. The annual fluxes was around -9.1×10^{15} mmol C yr^{-1} for the Southern Ocean waters[51].

The springtime phytoplankton blooms in the high-latitude oceanic regions reduce the surface CO_2 concentration. Higher values were observed during winter in the subpolar and polar waters of South Atlantic, North Pacific, North and South Atlantic Oceans. The seasonality in the fluxes was visible from the winter sources and summer sinks in the high-latitude areas of North Atlantic, North Pacific and Weddel Sea. This seasonality was accredited to the intense winter upwelling and increased summer photosynthesis. In tropical oceanic regions where the biological factors are comparatively weak, temperature determines the flux direction with CO_2 release from the ocean surface in summer and absorption in winter. A combination of the subtropical cooling and strong subpolar photosynthetic CO_2 consumption generates an intense sink in the subtropical convergence region. The major global CO_2 sinks were found to be located in the temperate and polar regions, whereas the equatorial region acted as a source. The Southern Ocean is a significant sink despite the upwelling regions around Antarctica[52]. The Atlantic Ocean was found to be the most intense sink with 60% of the global CO_2 uptake, while the Indian Ocean and Southern Ocean combined contributed by 20%. The Pacific equatorial belt was identified as a strong CO_2 source, which was balanced by the temperate sinks. Fluxes in the eastern equatorial Pacific, equatorial and subpolar waters, the northwestern Arabian Sea, Antarctic and the Sub-Arctic North Pacific coastal waters were found to be controlled by biological factors, whereas temperature factor dominated the subtropical gyre areas. The annual uptake of CO_2 by global oceans was estimated to be 50×10^{15} mmol C yr^{-1} (ref. 9).

Conclusion

The global ocean acts as a net CO_2 sink with flux value of 50×10^{15} mmol C yr^{-1}, with high-latitude areas behaving as sources of CO_2 to the atmosphere in winter and sinks in summer. Tropical oceans exhibit the reverse trend. This seasonal behaviour of fluxes in the subpolar and polar regions results from the intense winter upwelling and increased photosynthetic activity in summer. Temperature is the key regulating factor in the tropics where the biological forcing is weak. The western subarctic North Pacific is a source in winter influenced by the physical forcing and becomes a sink with the summer photosynthetic drawdown of CO_2 peaks. The western North Pacific, on the other hand, proved to be a strong sink with maximum absorption in winter. The Atlantic region was recognized as the strongest sink of –815 to –1295 mmol C m^{-2} yr^{-1} in the North Atlantic subtropical gyre, while the Pacific Ocean has been remained a neutral basin in terms of the CO_2 fluxes, since the intense outwards fluxes occurring in the equatorial belt are balanced by the sink zones in the temperate region. However, it tends to switch from an annual sink to a source as a consequence of the thermal anomalies in the North Pacific. The Indian Ocean and the Southern Ocean also contribute to the global sinks; however, the western sub-basin of the northern Indian Ocean is an annual net source with fluxes of 2.04×10^{15} mmol C yr^{-1}. The strong subtropical convergence zone acts as a strong sink, resulting from the occurrence of subtropical cooling and photosynthetic CO_2 intake in the subpolar oceans. The spatial and seasonal variability of the global CO_2 fluxes is triggered by the intensity of the physical and biological forcings as well as the thermal variations in particular oceanic regions. While the equatorial, subpolar, Antarctic and Sub-Arctic regions are dominated by the biological factors, the subtropical zones are influenced by the thermal component.

From studies conducted over different oceanic regions, it can be observed that the Indian Ocean exhibits a peculiarity in terms of CO_2 gas transfer. Even though this oceanic region contributes to the global CO_2 sinks, there is a contrasting nature of CO_2 fluxes in between the western and eastern sub-basins of the northern Indian Ocean, which can be better explained in terms of the contrasting trends in ocean primary productivity, freshwater and nutrient availability which govern the physical, chemical and biological processes in these waters. While major nutrient source is the river-water influx for BoB waters, the Arabian Sea is enriched with nutrients through the eolian dust fluxes from the deserts of Somalia and Arabia, especially iron which is the limiting nutrient in oceanic waters. The strong wind mixing of the surface waters along with the upwelling processes well distribute the available nutrients in the Arabian Sea, whereas the weak wind forcing and strong surface stratification restrict the nutrients distribution in BoB waters. Such contrasting trends between these two sub-basins of the Indian Ocean need to be analysed in detail both spatially and temporally using satellite as well as field data analysis in order to understand the biogeochemistry of these waters and its importance in regulating the carbon fluxes.

1. Chester, R., *Marine Geochemistry*, Blackwell Science Ltd, Oxford, UK, 2000, 2nd edn, p. 506.
2. Velasco, E. and Roth, M., Cities as net sources of CO_2: review of atmospheric CO_2 exchange in urban environments measured by eddy covariance technique. *Geogr. Compass*, 2010, **4**(9), 1238–1259; 10.1111/j.1749-8198.2010.00384.x.
3. Feely, R. A., Sabine, C. L., Takahashi, T. and Wanninkhof, R., Uptake and storage of carbon dioxide in the ocean: the global CO_2 survey. *Oceanography*, 2001, **14**(4), 18–32.
4. Zeebe, R. E., History of sea water carbonate chemistry, atmospheric CO_2 and ocean acidification. *Annu. Rev. Earth Planet. Sci.*, 2012, **40**, 141–165; doi:10.1146/annurev-earth-042711-105521.
5. Fletcher, S. E. M. *et al.*, Inverse estimates of the oceanic sources and sinks of natural CO_2 and the implied oceanic carbon transport. *Global Biogeochem. Cycles*, 2007, **21**, GB1010, 19; doi:10.1029/2006GB002751.
6. DOE, *Handbook of Methods for the Analysis of the Various Parameters of the Carbon Dioxide System in Sea Water*, *Version 2*,

United States Department of Energy (DOE), ORNL/CDIAC-74, 1994.
7. Buesseler, M., Bowles, M. and Joyce, K., US JGOFS Brochure, US JGOFS Planning and Data Management Office, Wooda Whole, Massachusetts, USA, 2013.
8. Caldera, K. and Wickett, M. E., Anthropogenic carbon and ocean pH. *Nature Brief Commun.*, 2003, **425**, 365.
9. Takahashi, T. *et al.*, Global sea–air CO_2 flux based on climatological surface ocean pCO_2, and seasonal biological and temperature effects. *Deep-Sea Res. II*, 2002, **49**, 1601–1622.
10. Ono, T., Saino, T., Kurita, N. and Sasaki, K., Basin-scale extrapolation of shipboard pCO_2 data by using satellite SST and Chl *a*. *Int. J. Remote Sensing*, 2004, **25**(19), 3803–3815.
11. Landschutzer, P., Gruber, M. and Bakker, D. C. E., Decadal variations and trends of the global ocean carbon sink. *Global Biogeochem. Cycles*, 2016, **30**, 1396–1417; https://doi.org/10.1002/2015GB005359.
12. Padhy, P. C. *et al.*, Estimation of partial pressure of carbon dioxide and air–sea fluxes in Hooghly estuary based on *in situ* and satellite observations. *J. Indian Soc. Remote Sensing*, 2016, **44**(1), 135–143; doi:10.1007/s12524-015-0459-z.
13. Millero, F., Lee, K. and Roche, M., Distribution of alkalinity in the surface oceans of the major oceans. *Mar. Chem.*, 1998, **60**, 111–130.
14. Goes, J. I., Saino, T., Oaku, H., Ishizaka, J., Wong, C. S. and Nojiri, Y., Basin scale estimates of sea surface nitrate and new production from remotely sensed sea surface temperature and chlorophyll. *Geophys. Res. Lett.*, 2000, **27**, 1263–1266.
15. Lee, K., Wanninkhof, R., Feely, R. A., Millero, F. J. and Peng, T. H., Global relationship of total inorganic carbon with temperature and nitrate in surface sea water. *Global Biogeochem. Cycles*, 2000, **14**, 979–994.
16. Sarma, V. V. S. S. *et al.*, Basin-scale pCO_2 distribution using satellite sea surface temperature, Chl *a*, and climatological salinity in the North Pacific in spring and summer. *Global Biogeochem. Cycles*, 2006, **20**, GB3005; doi:10.1029/2005GB002594.
17. Zhu, Y., Shag, S., Zhai, W. and Dai, M., Satellite-derived surface water pCO_2 and air–sea CO_2 fluxes in the northern South China Sea in summer. *Prog. Nat. Sci.*, 2009, **19**, 775–779.
18. Zui, T., Bangyong, B., Ziwei1, L. and Xiaofeng, Y., Satellite observations of the partial pressure of carbon dioxide in the surface water of the Huanghai Sea and the Bohai Sea. *Acta Oceanol. Sin.*, 2012, **31**(3), 67–73; doi:10.1007/s13131-012-0207-y.
19. Liu, T. W. and Xie, X., Ocean surface carbon dioxide fugacity observed from space. JPL Publication 14–15, National Aeronautics and Space Administration, Jet Propulsion Laboratory California Institute of Technology Pasadena, California, USA, 2014, p. 18.
20. Jang, E., Im, J., Park, G. and Park, Y., Estimation of fugacity of carbon dioxide in the East Sea using *in situ* measurements and Geostationary Ocean Color Imager satellite data. *Remote Sensing*, 2017, **9**(821), 23; doi:10.3390/rs9080821.
21. Stephens, M. P., Samuels, G., Olson, D. B., Fine, R. A. and Takahashi, T., Sea–air flux of CO_2 in the North Pacific using shipboard and satellite data. *J. Geophys. Res.*, 1995, **100**(C7), 13571–13583.
22. Cosca, C. E., Feely, R. A., Boutin, J., Etcheto, J., McPhaden, M. J., Chavez, F. P. and Strutton, P. G., Seasonal and interannual CO_2 fluxes for the central and eastern equatorial Pacific Ocean as determined from fCO_2–SST relationships. *J. Geophys. Res.*, 2003, **108**(C8), 3278; doi:10.1029/2000JC000677.
23. Takamura, T. R., Inoue, H. Y., Midorikawa, T., Ishii, M. and Nojiri, Y., Seasonal and inter-annual variations in pCO_2 sea and air–sea CO_2 fluxes in mid-latitudes of the western and eastern North Pacific during 1999–2006. *J. Meteorol. Soc. Jpn*, 2010, **88**(6), 883–898; doi:10.2151/jmsj.2010-602.
24. Dixit, A., Lekshmi, K., Bharti, R. and Mahanta, C., Basin scale estimation of partial pressure of carbon dioxide in case 1 waters of Bay of Bengal. In International Geoscience and Remote Sensing Symposium, Velencia, Spain, 23–27 July 2018.
25. Takahashi, T., Olaffson, J., Goddard, J. D., Chipman, D. W. and Sutherland, S. C., Seasonal variation of CO_2 and nutrients in the high-latitude surface oceans: a comparative study. *Global Biogeochem. Cycles*, 1993, **7**(4), 843–878.
26. Da Vila, M. G., Casiano, J. M. S. and Da Vila, E. F. G., Interannual variability of the upper ocean carbon cycle in the northeast Atlantic Ocean. *Geophys. Res. Lett.*, 2007, **34**, L07608; doi:10.1029/2006GL028145.
27. Körtzinger, A. and Duinker, J. C., Strong CO_2 emissions from the Arabian Sea during south-west monsoon. *Geophys. Res. Lett.*, 1997, **24**(14), 1763–1766.
28. Goet, C., Millero, F. J., OÕSullivan, D. W., Eischeid!, G., McCue, S. J. and Bellerby, R. G. J., Temporal variations of pCO_2 in surface seawater of the Arabian Sea in 1995. *Deep-Sea Res. I*, 1998, **45**, 609–623.
29. Sarma, V. V. S. S., Kumar, M. D. and George, M. D., The central and eastern Arabian Sea as a perennial source of atmospheric carbon dioxide. *Tellus B*, 1998, **50**, 179–184.
30. Sarma, V. V. S. S., Monthly variability in surface pCO_2 and net air–sea CO_2 flux in the Arabian Sea. *J. Geophys. Res.*, 2003, **108**(C8), 3255; doi:10.1029/2001JC001062.
31. Sarma, V. V. S. S. *et al.*, Carbon dioxide emissions from Indian monsoonal estuaries. *Geophys. Res. Lett.*, 2012, **39**, L03602, 5; doi:10.1029/2011GL050709.
32. Sarma, V. V. S. S. *et al.*, Sources and sinks of CO_2 in the west coast of Bay of Bengal. *Tellus B*, 2012, **64**, 10961; doi:10.3402/tellusb.v64i0.10961.
33. Valsala, V., Makyutov, S. and Murtugudde, R., A window for carbon uptake in the southern subtropical Indian Ocean. *Geophys. Res. Lett.*, 2012, **39**, 1–7; doi:10.1029/2012GL052857.
34. Sarma, V. V. S. S. *et al.*, Sea–air CO_2 fluxes in the Indian Ocean between 1990 and 2009. *Biogeosciences*, 2013, **10**, 7035–7052; doi:10.5194/bg-10-7035-2013.
35. Valsala, V. and Maksyutov, S., Interannual variability of air–sea CO_2 flux in the north Indian Ocean. *Ocean Dyn.*, 2013, **63**, 165–178; doi:10.1007/s10236-012-0588-7.
36. Preethi Latha, T. *et al.*, Estimation of air–sea CO_2 flux in the coastal waters of Visakhapatnam. *J. Indian Soc. Remote Sensing*, 2015, **43**(3), 647–652.
37. Valsala, V. and Murtugudde, R., Mesoscale and intraseasonal air–sea CO_2 exchanges in the Western Arabian Sea during boreal summer. *Deep Sea Res. I*, 2015, **103**, 101–113; doi:10.1016/j.dsr.2015.06.001.
38. Shanthi, R., Poornima, D., Naveen, M., Thangaradjou, T., Choudhury, S. B., Rao, K. H. and Dadhwal, V. K., Air–sea CO_2 flux pattern along the southern Bay of Bengal waters. *Dyn. Atmos. Oceans*, 2016, **76**, 14–28.
39. Midorikawa, T., Umedaa, T., Hiraishia, N., Ogawaa, K., Nemotoa, K., Kuboa, N. and Masao, I., Estimation of seasonal net community production and air–sea CO_2 flux based on the carbon budget above the temperature minimum layer in the western subarctic North Pacific. *Deep-Sea Res. I*, 2002, **49**, 339–362.
40. Feely, R. A., Wanninkhof, R., McGillis, W., Carr, M. E. and Cosca, C. E., Effects of wind speed and gas exchange parameterizations on the air–sea CO_2 fluxes in the equatorial Pacific Ocean. *J. Geophys. Res.*, 2004, **109**, C08S03, 10; doi:10.1029/2003JC001896.
41. Feely, R. A., Takahashi, T., Wanninkhof, R., McPhaden, M. J., Cosca, C. E., Sutherland, S. C. and Carr, M., Decadal variability of the air–sea CO_2 fluxes in the equatorial Pacific Ocean. *J. Geophys. Res.*, 2006, **111**, C08S90, 1–16; doi:10.1029/2005JC003129.
42. Valsala, V., Maksyutov, S., Telszewski, M., Nakaoka, S., Nojiri, Y., Ikeda, M. and Murtugudde, R., Climate impacts on the structures of the North Pacific air–sea CO_2 flux variability. *Biogeosciences*, 2012, **9**, 477–492; doi:10.5194/bg-9-477-2012.

43. Valsala, V., Roxy, M., Ashok, K. and Murtugudde, R., Spatio-temporal characteristics of seasonal to multidecadal variability of pCO_2 and air–sea CO_2 fluxes in the equatorial Pacific Ocean. *J. Geophys. Res.: Oceans*, 2014, **119**, 8987–9012; doi:10.1002/2014JC010212.
44. Sutton, A. J., Wanninkhof, R., Sabine, C. L., Feely, R. A., Cronin, M. F. and Weller, R. A., Variability and trends in surface sea water pCO_2 and CO_2 flux in the Pacific Ocean. *Geophys. Res. Lett.*, 2017, **44**, 5627–5636; doi:10.1002/2017GL073814.
45. Olsen, A., Bellerby, R. G. J., Johannessen, T., Omar, A. M. and Skjelvan, I., Interannual variability in the wintertime air–sea flux of carbon dioxide in the northern North Atlantic, 1981–2001. *Deep-Sea Res. I*, 2003, **50**, 1323–1338.
46. Bates, N. R., Interannual variability of the oceanic CO_2 sink in the subtropical gyre of the North Atlantic Ocean over the last 2 decades. *J. Geophys. Res.*, 2007, **112**, 26; doi:10.1029/2006JC003759.
47. Oliveiraa, R. R., Pezzia, L. P., Souzab, R. B., Santinia, M. F., Cunhac, L. C. and Pachecod, F. S., First measurements of the ocean–atmosphere CO_2 fluxes at the Cabo Frio upwelling system region, Southwestern Atlantic Ocean. *Continent. Shelf Res.*, 2019, **181**, 135–142; https://doi.org/10.1016/j.csr.2019.05.008.
48. Orselli, I. B. M., Kerra, R., Azevedoa, J. L. L., Galdinoa, F., Araujoe, M. and Garcia, C. A. E., The sea–air CO_2 net fluxes in the South Atlantic Ocean and the role played by Agulhas eddies. *Prog. Oceanogr.*, 2019, **170**, 40–52; https://doi.org/10.1016/j.pocean.2018.10.006.
49. Takahashi, T., Freely, R. A., Weiss, R. F., Wanninkhof, R. H., Chipman, D. W., Sutherland, S. C. and Takahashi, T. T., Global air–sea flux of CO_2: an estimate based on measurements of sea–air pCO_2 difference, Colloquium Paper. *Proc. Natl. Acad. Sci. USA*, 1997, **94**, 8292–8299.
50. Zhai, W., Dai, M., Cai, W., Wang, Y. and Hong, H., The partial pressure of carbon dioxide and air–sea fluxes in the northern South China Sea in spring, summer and autumn. *Mar. Chem.*, 2005, **96**, 86–97.
51. McNeil, B. I., Metzl, N., Key, R. M., Matear, R. J. and Corbiere, A., An empirical estimate of the Southern Ocean air–sea CO_2 flux. *Global Biogeochem. Cycles*, 2007, **21**, GB3011; doi:10.1029/2007GB002991.
52. Gray, A. R. *et al.*, Autonomous biogeochemical floats detect significant carbon dioxide outgassing in the high-latitude Southern Ocean. *Geophys. Res. Lett.*, 2018, **45**(17), 9049–9057; https://doi.org/10.1029/2018GL078013.
53. Mongwe, N. P., Vichi, M. and Monteiro, M. S., The seasonal cycle of pCO_2 and CO_2 fluxes in the Southern Ocean: diagnosing anomalies in CMIP5 earth system models. *Biogeosciences*, 2018, **15**, 2851–2872; https://doi.org/10.5194/bg-15-2851-2018.
54. Murtugudde, R., Seager, R. and Thoppil, P., Arabian Sea response to monsoon variations. *Paleoceanography*, 2007, **22**, PA4217; doi:10.1029/2007PA001467.
55. Valsala, V., Different spreading of Somali and Arabian coastal upwelled waters in the northern Indian Ocean: a case study. *J. Phys. Oceanogr.*, 2009, **65**, 803–816; doi:https://doi.org/10.1007/s10872-009-0067-z.
56. Sreeush, M. G., Saran, R., Valsala, V., Pentakotta, S., Prasad, K. V. S. R. and Murtugudde, R., Variability, trend and controlling factors of ocean acidification over Western Arabian Sea upwelling region. *Mar. Chem.*, 2019, **29**, 14–24; https://doi.org/10.1016/j.marchem.2018.12.002.
57. Vinayachandran, P. N., Murty, V. S. N. and Babu, V. R., Observations of barrier layer formation in the Bay of Bengal during summer monsoon. *J. Geophys. Res.*, 2002, **107**(C12), 8018, 19.1–19.9; doi:10.1029/2001JC000831.
58. Murtugudde, R. and Busalacchi, A. J., Interannual variability of the dynamics and thermodynamics of the tropical Indian Ocean. *J. Climate*, 1999, **12**, 2300–2326; doi:10.1175/1520-0442.
59. Vinayachandran, P. N. and Mathew, S., Phytoplankton bloom in the Bay of Bengal during the northeast monsoon and its intensification by cyclones. *Geophys. Res. Lett.*, 2003, **30**(11), 1572, 26.1–26.4; doi:10.1029/2002GL016717.
60. Vinayachandran, P. N., Chauhan, P., Mohan, M. and Nayak, S., Biological response of the sea around Sri Lanka to summer monsoon. *Geophys. Res. Lett.*, 2004, **31**, L0102, 1–4; doi:10.1029/2003GL018533.
61. Vinayachandran, P. N., McCreary Jr, J. P., Hood, R. R. and Kohler, K. E., A numerical investigation of the phytoplankton bloom in the Bay of Bengal during northeast monsoon. *J. Geophys. Res.*, 2005, **110**, C12001, 1–14; doi:10.029/2005JC002966.
62. Susanto, R., Gordon, A. L. and Zheng, Q., Upwelling along the coasts of Java and Sumatra and its relation to ENSO. *J. Geophys. Res. Lett.*, 2001, **28**, 1599–1602; doi:10.1029/2000GL011844.
63. Chakraborty, K., Valsala, V., Gupta, G. V. M. and Sarma, V. V. S. S., Dominant biological control over upwelling on pCO_2 in sea east of Sri Lanka. *J. Geophys. Res.: Biogeosci.*, **123**, 3250–3261; doi:10.1029/2018JG004446.
64. McCreary, J. *et al.*, Biophysical processes in the Indian Ocean. *Geophys. Monogr. Ser.*, 2009, **185**, 9–32; https://doi.org/10.1029/2008GM000768.

Received 14 February 2019; revised accepted 18 December 2020

doi: 10.18520/cs/v121/i5/626-640